

**APPROVAL**

**INVESTIGATION ON INDENTATION CREEP PERFORMANCE OF  
CARBON NANOTUBES REINFORCED TIN-58BISMUTH  
COMPOSITES**

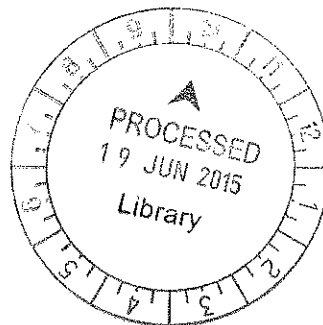
by

Tan Chin Keat

A project dissertation submitted to the  
Faculty of Science, Technology, Engineering & Mathematics  
INTI INTERNATIONAL UNIVERSITY  
in partial fulfilment of the requirement for the  
Bachelor of Engineering (Hons) in  
Mechanical Engineering

Approved:

\_\_\_\_\_  
Dr How Ho Cheng  
Project Supervisor



INTI INTERNATIONAL UNIVERSITY  
NILAI, NEGERI SEMBILAN

January 2015

## DECLARATION

I, the undersigned, hereby declare that this report is my own independent work except as specified in the references and acknowledgements. I have not committed plagiarism in the accomplishment of this work, nor have I falsified and/or invented the data in my work. I am aware of the University regulations on Plagiarism. I accept the academic penalties that may be imposed for any violation.

Signature ..... *Tan Chin Keat* .....

Name ..... TAN CHIN KEAT .....

Matrix No. .... I 11008577 .....

Date ..... 29<sup>th</sup> MAY 2015 .....

## ABSTRACT

Low concentration of carbon nanotubes were added into eutectic Sn-58Bi solder alloy with the intention to improve the creep performance of the alloy. The solder alloy was produced using powder metallurgy route. Prior to the synthesis of the solder alloy and the composites, the effect of powders loading modes and rotational speeds of the V-shape mixer on the mixing uniformity were studied. The microstructure of the solder alloy and the composites were also examined under the optical microscope to observe the effect of sintering. Further microstructure characterization was performed using the scanning electron microscope as well as the energy dispersive X-ray analysis. Differential scanning calorimetry analysis was also performed on the powders mixtures to study the reactions that occurred during the sintering process. Sargent-Ashby creep model was then used to characterize the creep stress exponent of the solder alloy and the carbon nanotubes reinforced composites. Results from the experiment showed that the addition of small amount of carbon nanotubes of up to 0.2wt% was sufficient to lead to an improvement in the creep performance of the eutectic Sn-58Bi solder material. However, the improvement was not evident in the 0.5wt% and 1.0wt% composite samples due to the agglomeration of carbon nanotubes.

## ACKNOWLEDGEMENTS

The author would like to take this opportunity to extend his heartfelt gratitude to his project supervisor Dr How Ho Cheng, Department of Mechanical Engineering, INTI International University for always generously sharing his knowledge and providing continuous support and guidance throughout the course of this project.

The author would also like to convey his sincere regards to INTI International University for supporting this project with an internal grant and providing the equipment required for the project.

The author is also thankful to Dr Muralithran A/L Govindan Kutty, Department of Restorative Dentistry, University of Malaya for providing the carbon nanotubes needed for this project.

The author would also like to express his special thanks to the Department of Mechanical Engineering lab technicians, Mr Ravindran Sayagaran, Mr Aminuddin Shah and Miss Mazlia Abdul Holit, for their help during the project execution.

Last but not least the author would like to extend his appreciation to those who have directly or indirectly provided supports and helps in this study.

## DEDICATION

This thesis is dedicated to my parents who have never stop in giving of themselves to raise me up, and also to my beloved sisters who always encourage me when things look bleak in my life.

# TABLE OF CONTENTS

DECLARATION.....	i
ABSTRACT .....	ii
ACKNOWLEDGEMENTS.....	iii
DEDICATION.....	iv
LIST OF FIGURES .....	viii
LIST OF TABLES.....	xi
LIST OF ABBREVIATIONS.....	xii
NOMENCLATURE .....	xiii
CHAPTER 1           INTRODUCTION.....	1
1.1. Background.....	1
1.2. Problem Statement.....	2
1.3. Objectives of the Research .....	2
1.4. Scope of the Research.....	3
1.5. Report Organization.....	3
CHAPTER 2           LITERATURE REVIEW .....	4
2.1. Brief History of Semiconductor Industry .....	4
2.1.1. Moore's Prediction on Semiconductor .....	4
2.1.2. Transition From Pb-based to Pb-free Solders.....	4
2.2. Development of Pb-free solders .....	5
2.2.1. SAC solders .....	5
2.2.2. Sn-Zn solders .....	6
2.2.3. Sn-Bi solders.....	7
2.3. Creep.....	8
2.3.1. Understanding creep and its importance.....	8
2.3.2. Creep and semiconductor failures .....	8
2.3.3. Models developed for creep curves .....	13
2.3.4. Comparison between different types of creep tests .....	15

2.3.5.	Structural changes in material during creep .....	17
2.3.6.	Creep studies on Sn and Bi containing solder alloys and their composites .....	18
2.4.	Nanoparticle Reinforced Composite Solders.....	20
2.4.1.	CNT as reinforcement for solder .....	20
2.4.2.	Electrical Percolation Threshold of CNT .....	21
CHAPTER 3	METHODOLOGY & EXPERIMENTAL PROCEDURES ...	24
3.1.	Materials and Powder Metallurgy .....	24
3.1.1.	Materials .....	25
3.1.2.	Powder Mixing .....	26
3.1.3.	Powder Compaction.....	29
3.1.4.	Powder Sintering .....	31
3.2.	Microstructure characterization of composites.....	32
3.2.1.	Optical Microscopy .....	32
3.2.2.	Secondary Electron Microscopy.....	33
3.3.	Indentation Creep Performance .....	34
3.4.	Differential Scanning Calorimetry (DSC).....	36
3.5.	Experimental Procedure.....	36
3.5.1.	Powder Metallurgy .....	36
3.5.2.	Characterization of microstructure and Vickers hardness test .....	45
CHAPTER 4	RESULTS AND DISCUSSIONS.....	46
4.1.	Effect of initial loading mode to efficiency of mixing .....	46
4.2.	Effect of speed of rotation of V-mixer to efficiency of mixing.....	48
4.3.	Microstructure of post-sintered solder alloy and MWCNT-reinforced composites .....	50
4.3.1.	Optical microscope images.....	50
4.3.2.	SEM analysis .....	51
4.4.	DSC analysis.....	56

4.5. Creep Investigation.....	60
4.5.1. Change in indentation diagonal length with time.....	60
4.5.2. Determination of Norton stress exponent, n.....	64
4.5.3. Creep comparison between eutectic Sn-58Bi solder alloy and MWCNT-reinforced composites .....	69
CHAPTER 5           CONCLUSION AND FUTURE WORK.....	75
5.1. Conclusion.....	75
5.2. Recommendations & Future Work.....	75
REFERENCES .....	77
APPENDIX A   PROJECT GANTT CHART.....	87
APPENDIX B   INVESTIGATION ON EFFICIENCY OF POWDER MIXING PROCESS - EXPERIMENT DATA.....	88



## LIST OF FIGURES

Caption	Page No.
Figure 2.2.1 (a) SAC Ternary Phase Diagram and (b) Sn-rich corner	5
Figure 2.2.2 Sn-Bi Phase Diagram	7
Figure 2.3.1 Possible locations of solder interface crack	11
Figure 2.3.2 Possible locations of cracks at IMC layer of solder joints	12
Figure 2.3.3 Possible crack location at the bulk of solder	13
Figure 2.3.4 Strain vs time creep curves under constant load and constant stress	14
Figure 2.4.1 DC electrical conductivity of pure PMMA and different types of CNTs	21
Figure 2.4.2 Electrical conductivity of PAM-MWCNT composites versus alternating current frequency for 0.3%, 1.0% and 3.0% MWCNT contents	22
Figure 3.1.1 Processes involved in powder metallurgy	26
Figure 3.1.2 Portillo's compartment model to determine the effect of loading mode to mixing efficiency	29
Figure 3.1.3 A typical powder compacting process	30
Figure 3.2.1 Typical parts of a light microscope	32
Figure 3.2.2 Typical parts of SEM	33
Figure 3.3 Vickers hardness tester	34
Figure 3.4.1 Mettler Toledo Weighing Balance ML303E/02 used for measuring the weight of powders	37
Figure 3.4.2 CAPSULCN International Co.Ltd V241014 V-mixer used for mixing the powders	38
Figure 3.4.3 A fixed-volume small container used for containing the powders for weight measurements	38
Figure 3.4.4 Plunger and die used for compacting the powder mixtures	41
Figure 3.4.5 Plunger and die placed under the hydraulic press machine with the powder mixture inside the die	41

Figure 3.4.6 ezyLift Hydraulic Shop Crane used for compacting the powder mixtures	42
Figure 3.4.7 Compacted powder mixture	42
Figure 3.4.8 Nabertherm 8kW oven used for sintering the green compacts	43
Figure 3.4.9 Post-sintered solid form of Sn-58Bi	43
Figure 3.4.10 Silicon mold made with intention to hold the post-sintered solid	44
Figure 3.4.11 Different grits of silicon carbide paper for grinding purpose	44
Figure 3.4.12 Polishing solutions ranging from 6 micron to 0.05 micron	45
Figure 4.1.1 Comparison between changes in STD with mixing time for Top-Bottom and Left-Right initial loading modes	47
Figure 4.2.2 Comparison between changes in STD with mixing time for five different speeds of rotation	49
Figure 4.3.1 SEM image of Sn-58Bi-0.2CNT powder mixture with 150 X magnification	51
Figure 4.3.2 SEM image of Sn-58Bi-0.2CNT powder mixture with 600 X magnification	52
Figure 4.3.3 EDX analysis of Sn-58Bi-0.2CNT powder mixture	52
Figure 4.3.4 SEM image of the Sn-58Bi post-sintered solid with 0.2wt% MWCNT reinforcement (100X magnification)	53
Figure 4.3.5 SEM image of the Sn-58Bi post-sintered solid with 0.2wt% MWCNT reinforcement with 1000X magnification	54
Figure 4.3.6 SEM image of the voids in Sn-58Bi post-sintered solid with 0.2wt% MWCNT reinforcement (300X magnification)	54
Figure 4.3.6 SEM image of MWCNT (200000X Magnification)	55
Figure 4.4.1 DSC Data obtained from Sn-58Bi powders	56
Figure 4.4.2 DSC Data obtained from Sn-58Bi-0.2MWCNT powders	58
Figure 4.4.3 Image of Sn-58Bi-0.2MWCNT compacted solid under optical microscope with 100X magnification	59
Figure 4.5.1 Change in average diagonal length, $D_{avg}$ with dwell time for Sn-58Bi	61

Figure 4.5.2 Change in average diagonal length, $D_{avg}$ with dwell time for Sn-58Bi-0.1MWCNT specimen	61
Figure 4.5.3 Change in average diagonal length, $D_{avg}$ with dwell time for Sn-58Bi-0.2MWCNT specimen	62
Figure 4.5.4 Change in average diagonal length, $D_{avg}$ with dwell time for Sn-58Bi-0.5MWCNT specimen	62
Figure 4.5.5 Change in average diagonal length, $D_{avg}$ with dwell time for Sn-58Bi-1.0MWCNT specimen	63
Figure 4.5.6 Plotting $d$ against the Hv in double logarithmic scale for Sn-58Bi	66
Figure 4.5.7 Plotting $d$ against the Hv in double logarithmic scale for Sn-58Bi-0.1MWCNT	66
Figure 4.5.8 Plotting $d$ against the Hv in double logarithmic scale for Sn-58Bi-0.2MWCNT	67
Figure 4.5.9 Plotting $d$ against the Hv in double logarithmic scale for Sn-58Bi-0.5MWCNT	67
Figure 4.5.10 Plotting $d$ against the Hv in double logarithmic scale for Sn-58Bi-1.0MWCNT	68
Figure 4.5.11 Direct comparison of change in average diagonal length of all the materials under study with dwell time	70
Figure 4.5.12 Direct comparison of $\ln d$ vs $\ln Hv$ of all the materials under investigation	70
Figure 4.5.13 Mixed Sn-58Bi-0.5MWCNT	72
Figure 4.5.14 Mixed Sn-58Bi-1.0MWCNT	72

## LIST OF TABLES

Caption	Page No.
Table 2.3.1 Typical JEDEC Tests for Component and Assembly Level Testing	9
Table 3.1.1 Information on materials used for the research	25
Table 3.1.2 Types of mixers suitable for different types of materials	27
Table 3.2.1 Variation in magnification of optical microscope with numerical aperture and working distance	33
Table 4.1.1 Changes in STD with mixing time for different initial loading modes	46
Table 4.2.1 Changes in STD with mixing time for different speeds of rotation	48
Table 4.3.1 Microstructure of samples before and after sintering	50
Table 4.5.1 Average diagonal length, $D_{avg}$ of indentation for eutectic Sn-58Bi solder alloy and MWCNT-reinforced composite for different dwell time	60
Table 4.5.2 Average diagonal length, $D_{avg}$ of indentation for eutectic Sn-58Bi solder alloy and MWCNT-reinforced composite for different dwell time	64
Table 4.5.3 Rate of change in average diagonal length, $\dot{d}$ for different dwell time, T	65
Table 4.5.4 Logarithmic values of $Hv$ and $\dot{d}$ for the eutectic Sn-58Bi solder alloy and the MWCNT-reinforced composites	65
Table 4.5.5 Norton's creep exponent for the materials under investigation	69
Table 4.5.6 Standard deviations of average diagonal lengths, $D_{avg}$ obtained in the indentation hardness test	73
Table 4.5.7 Standard deviations of hardness obtained in the indentation hardness test	74

## LIST OF ABBREVIATIONS

EU	European Union
WEEE	Waste Electrical and Electronic Equipment
RoHS	Restriction of Hazardous Substances
CNT	Carbon Nanotubes
SAC	Stannum-Argentum-Cuprum / Tin-Silver-Copper
MWCNT	Multi-walled Carbon Nanotubes
SWCNT	Single-walled Carbon Nanotubes
CSR	Constant Strain Rate
PAM	Polyacrylamide
STD	Standard deviation
SEM	Secondary Electron Microscopy
DSC	Differential Scanning Calorimetry
PMMA	Poly-methyl methacrylate
DWCNT	Double-walled Carbon Nanotubes

## NOMENCLATURE

<i>Symbol</i>	<i>Definition</i>
<i>Pb</i>	Plumbum / Lead
<i>Sn</i>	Stannum / Tin
<i>Bi</i>	Bismuth
<i>Sb</i>	Antimony
<i>Cu</i>	Cuprum/Copper
<i>Ni</i>	Nickel
<i>wt%</i>	Weight percentage
<i>Ag</i>	Argentum/Silver
<i>In</i>	Indium

# CHAPTER 1

## INTRODUCTION

### 1.1. Background

The eutectic Sn-40Pb solder alloy was once a widely used material for electronic assemblies in the semiconductor industry until global environmental concerns in the beginning of the third millennium spark countries around the world to enforce laws to battle environmental issues and pollutions (Hansen, 2010). With the creation of WEEE Directive in 2002 (ARCADIS ECOLAS & RPA, 2008) and the establishment and enforcement of RoHS Directive by EU in 2003 (Neill, 2004), the usage of several hazardous substances in semiconductor devices, including Pb, are banned. Consequently, the inevitable transition from leaded to lead free solders has forced the semiconductor manufacturers to start looking into possible candidates which are able to replace the Pb-based solders that has been used for many decades. Various studies (Reinikainen, 1999; Mathew et al., 2005) have been performed to search for the suitable solder alternative to replace the Sn-40Pb solder alloy which is cheap, has good solderability and reliability, and exhibit a low melting temperature of 183°C.

From the research initiated by three semiconductor manufacturers in Europe (Infineon Technologies et al., 2001), the Sn-Ag-Cu solder material, or also known as SAC, was found to be the most suitable primary alternative to replace the conventional Sn-40Pb solder material.

The transition from Pb-containing solder to the Pb-free SAC solder means that the soldering reflow temperature in the assembly process needs to be changed to a higher temperature of 217°C due to the different melting point exhibited by the SAC solder compared to the conventional solder material. The change in the soldering reflow temperature has escalated the risk of temperature-induced defects in electrical and electronic components, with dynamic warpage becoming a major concern in semiconductor industry. As the development of silicon chips is growing in line with prediction made by Moore's law (Ward, 2011), the size of the microelectronic devices will continue to shrink. The thinner silicon die and coreless polymer substrate will further increase the risk of dynamic warpage in semiconductor devices. To alleviate

the risk of temperature-induced defects in semiconductor devices, semiconductor industry has started to develop other solder materials with low melting temperature. Among the possible candidates for low melting solder includes the eutectic Sn-58Bi solder alloy, which has a low melting temperature of 139°C.

## **1.2. Problem Statement**

The eutectic Sn-58Bi solder has much lower melting point if compared to the conventional Sn-40Pb and the SAC solders and is therefore expected to be able to reduce the dynamic warpage issue during the soldering reflow process by allowing a lower reflow temperature during component assemblies. However, due to the relatively low melting point of 139°C exhibited by the eutectic Sn-58Bi solder alloy, the material has high homologous temperature of 0.72 even at room temperature of 25°C. At this high homologous temperature, creep is the most vital deformation mechanism (Mahmudi et al., 2013). The remedy proposed to improve the creep performance of the solder is to add CNT into the eutectic Sn-58Bi solder. As CNT exhibit superior Young's modulus and electrical conductivity, the CNT-reinforced Sn-58Bi composites are expected to deliver improved creep performance and electrical properties.

## **1.3. Objectives of the Research**

This paper serves to evaluate the properties of both eutectic Sn-58Bi solder and CNTs reinforced Sn-58Bi composites to verify the possibility of using it as an alternative solder material for low temperature soldering. The objectives of the study include:

- To synthesize Sn-58Bi composite materials with different CNT reinforcements using powder metallurgy route
- To perform microstructure characterization of the Sn-58Bi CNT reinforced composites using optical and secondary electron microscopy
- To investigate the indentation creep performance of the Sn-58Bi CNT reinforced composites
- To analyze the indentation creep performance of the composites in relation to the microstructure characterization of the composites



#### **1.4. Scope of the Research**

This thesis focuses on improving the creep performance of the eutectic Sn-58Bi solder alloy by using only MWCNT as reinforcement. The electrical properties of the MWCNT-reinforced Sn-58Bi composites were not studied. However, it is expected that if the reinforcement with MWCNT can yield a composite with good electrical properties, then using SWCNT as the reinforcement material will give a composite with even better electrical performance (Al-Osaimi & Alhosiny, 2013). The author cautions that the results obtained from the experiments performed in this study reflect the creep resistance of the composites with agglomeration of MWCNT in the samples, and therefore the creep performance of the composites may be improved if the MWCNT can be pre-treated to prevent agglomeration of the MWCNT during the powder mixing process.

In addition, although creep of solder alloys can be studied using various methods, the creep performance of the composites in this study was investigated using only indentation creep. The results from indentation creep test, however, have been previously proved to give similar results with the conventional creep test (Mahmudi, R. et al., 2007).

#### **1.5. Report Organization**

This thesis consists of five chapters. Chapter 1 presents the background and motivation behind the study, the problem statement and the scope of the analysis. To perform the study, research on previous works related to semiconductor failure modes and Pb-free materials as well as indentation creep has been reviewed and the analysis on these works will be covered in Chapter 2. Chapter 3 describes the methodology used to perform the investigations, which includes using powder metallurgy route to synthesize the composite and Vickers hardness tester to determine the indentation creep performance of the composite. In Chapter 4, the results obtained from the experiments are shown and are analysed in details. Chapter 5 summarizes all the findings and at the same time presents some recommendation and suggestions for future works.

## CHAPTER 2

### LITERATURE REVIEW

#### 2.1. Brief History of Semiconductor Industry

##### 2.1.1. *Moore's Prediction on Semiconductor*

Since its inception, the semiconductor industry has made phenomenal progress, with the costs reducing and the performance improving, the inevitable miniaturization of the electrical and electronics components allow devices such as mobile phones and computers to shrink in size. Moore (1965) predicted that the number of components that can be fitted onto an integrated circuit will continue to increase with the unit cost keep decreasing, and he also estimated that starting from 1975 the number of components that can be put on a single chip for the same cost will double every two years (Pumelt, 2003). The development of the silicon chip to date is still growing in line with Moore's prediction although more than 40 years has passed (Ward, 2011). With the number of transistors manufactured every year is expected to increase following Moore's Law in the near future and the size of the components getting smaller, there has been growing concern over the quality and reliability of the electronic components and devices. The transition from Pb-based solders to Pb-free solders in semiconductor industry due to the banning of lead usage since 2003 just got the semiconductor manufacturers out of the frying pan, into the fire.

##### 2.1.2. *Transition From Pb-based to Pb-free Solders*

Pb-based solders once dominated the semiconductor industry as the most widely used solder material due to their low cost, good solderability and reliability, and low melting temperature. However, usage of lead in semiconductor devices has been limited since the enforcement of RoHS Directive by EU in 2003 due to environmental concerns. Even though exemption has been granted for certain devices such as servers, storage and storage array systems up to the year of 2010, the banning of Pb means that development of new Pb-free solders is inevitable, with semiconductor manufacturers such as Infineon Technologies, Philips Semiconductors and STMicroelectronics began to develop the Pb-free SAC solder from as early as 2001 before the enforcement of RoHS Directive (Infineon Technologies et al., 2001).

## 2.2. Development of Pb-free solders

The new Pb-free solders have to meet requirements in several aspects, which include wettability, IMC formation, ductility, reliability, melting temperature as well as mechanical performance (Kotadia et al., 2014). Zeng et al. (2012) have reviewed the characteristics of some of the potential candidates for Pb-free solders, though their focus is being placed on high temperature solders. Few of the potential low melting temperature Pb-free solder to replace the leaded solder which have been identified to date include Sn-Ag-Cu (SAC), Sn-9Zn, and Sn-58Bi.

### 2.2.1. SAC solders

Eutectic and near-eutectic SAC alloys have low creep rate and show satisfying strength and ductility at the solder joints formed, which made them to be the primary candidate for replacing the conventional Sn-Pb solder alloys (Anderson & Wallerer, 2007). When the solder alloys are being placed in decreased thermal cycling temperature range, SAC shows improved results during the thermal fatigue tests if compared to the Sn-Pb alloys (Qi & Zbrzezny, 2004). Figure 2.2.1(a) shows the ternary phase diagram of SAC.

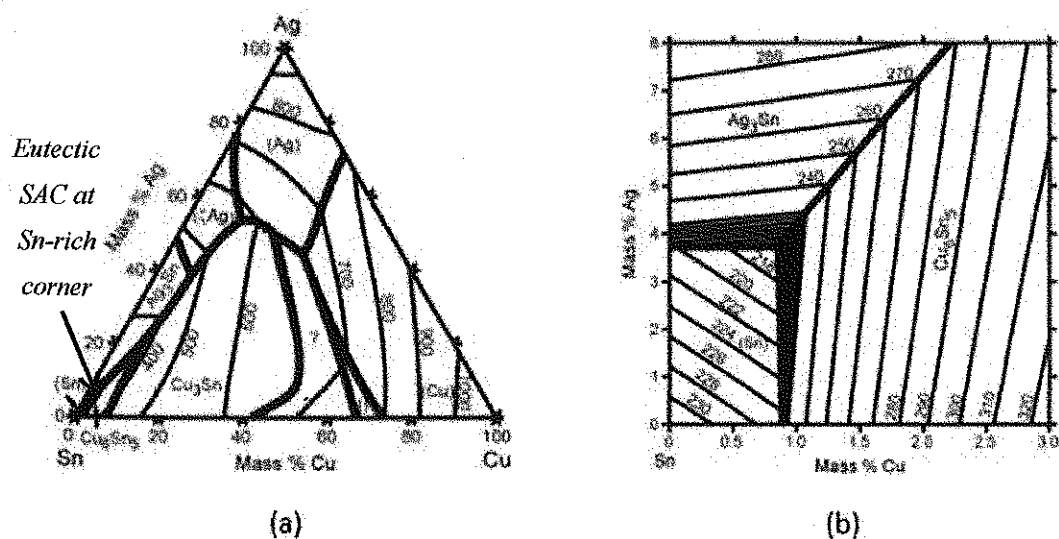


Figure 2.2.1 (a) SAC Ternary Phase Diagram and (b) Sn-rich corner

(Source : Moon & Boettinger, 2000)

Eutectic SAC alloys have composition of Sn-3.8Ag-0.7Cu (Anderson & Walleser, 2007). SAC solders developed to date are located in the Sn-rich corner of SAC ternary phase diagram as shown in Figure 2.2.1(b), with composition of Sn-(2.0-4.0 wt.%)Ag-(0.5-1.0 wt.%)Cu (Anderson & Foley, 2001). When SAC solders are joined with Cu substrate, the  $\text{Cu}_6\text{Sn}_5$  IMC was observed first with a very thin layer of  $\text{Cu}_3\text{Sn}$  forming at a later stage (Kivilahti, 1996). As time passes, the  $\text{Cu}_6\text{Sn}_5$  phase will dominate the solder joint component and grows at a very fast rate (Kim & Tu, 1995; Ghosh, 2000). During ageing, the  $\text{Cu}_3\text{Sn}$  phase will grow significantly and its behaviour during the growth may have vital impact on the reliability of the joint formed due to voids formation may occur in the  $\text{Cu}_3\text{Sn}$  layer (Tu, 2007). During SAC soldering, melting temperature of  $217^\circ\text{C}$  is being used during soldering reflow process. This reflow temperature is higher than the temperature used for Pb-Sn which is  $183^\circ\text{C}$  (Moon & Boettinger, 2000). Due to the higher soldering reflow temperature of SAC solders, dynamic warpage issue in the components during the reflow process has become one of the major concerns in semiconductor industry.

### 2.2.2. Sn-Zn solders

Eutectic Sn-Zn solder alloys have melting temperature of  $198^\circ\text{C}$  which is very close to the  $183^\circ\text{C}$  melting temperature exhibited by the Sn-Pb solders. Sn-Zn solder alloys are therefore considered as one of the potential Pb-based solders replacement candidate (Islam & Chan, 2005; Shiue & Tsay 2003; McCormark, 1994). At eutectic composition, Sn-Zn solders show higher mechanical strength and lower cost compared to the traditional Pb-based solders. However, Zn can be easily oxidized if not handled carefully during the assembly process, and with oxidation occurring, this means that the wettability of the solders will decrease due to the oxide layer formed. For certain cases, special fluxes and additional precautions are taken into consideration during the soldering reflow process (Rahn, 1993; Yu & Xie, 2004; Zhao & Ma, 2009; McCormark & Jin, 1994). The addition of Bi was found to be able to reduce the surface tension of the Sn-Zn solders (Bukat & Moser, 2010). Besides, the wettability of Sn-Zn solder alloys can be improved by doping the solders with Ag (Takemoto & Funaki, 2000), which at the same time can improve its ductility (McCormark & Jin, 1994).

### 2.2.3. Sn-Bi solders

In most solder alloys, Sn is used because it has greater tensile strength and shear strength. The Bi element itself has good wettability. When 58 wt.% of Bi is added into Sn, a eutectic solder alloy with a relatively low melting temperature is formed. Figure 2.2.2 shows the phase diagram of the Sn-Bi system.

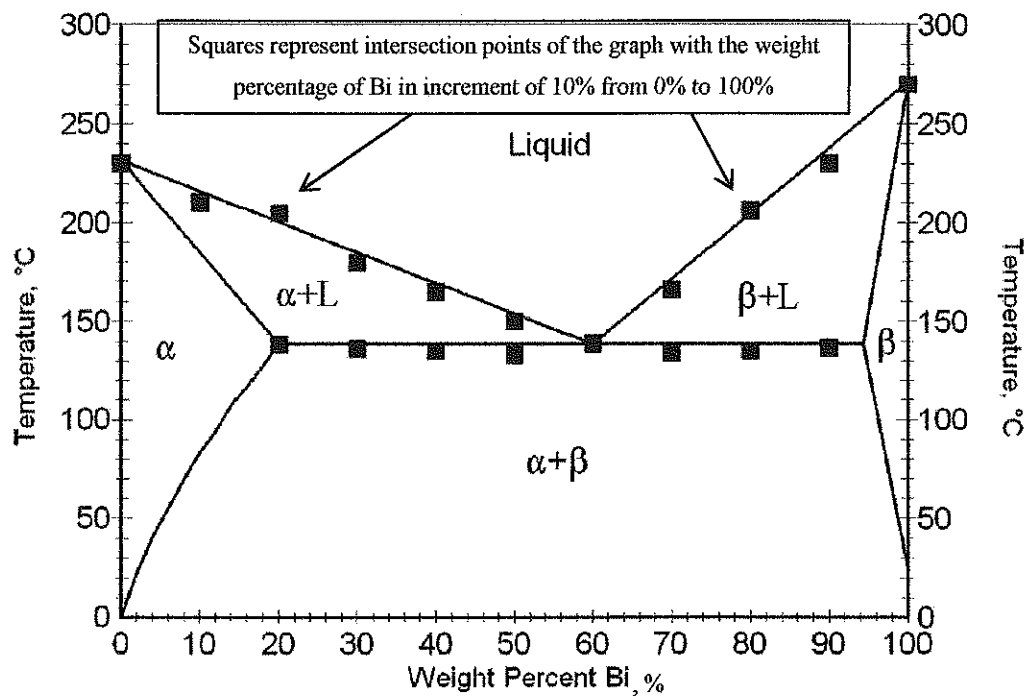


Figure 2.2.2 Sn-Bi Phase Diagram

(Source : K Street Studio, 2014)

The Sn element has a melting temperature of 231.9°C, while the melting temperature of the Bi element is 271°C. The eutectic composition of these 2 elements, however, has melting temperature of 139°C, which is quite low when compared to the traditional Sn-Pb solders. In addition, at room temperature, Sn-Bi solders show improved yield and fracture strength if compared with Sn-Pb solders (Hua & Mei, 1999). The low melting temperature of the eutectic solder alloy means that the soldering reflow can be performed at a lower temperature. The lower soldering temperature will not only help to save operational cost which can later be used for research and development purpose, but also reduce the risk of dynamic warpage of the components in the device during soldering reflow. Various studies have been

performed to evaluate the intermetallic growth at the interfaces between the SnBi solder and Cu substrate (Shang et al., 2013; Zhang et al., 2010). Similar to SAC solders, the Sn-58Bi solder alloys form  $\text{Cu}_6\text{Sn}_5$  IMC when they are being soldered onto a Cu substrate, and the subsequent ageing will cause  $\text{Cu}_3\text{Sn}$  to form. Due to their advantages, various studies on Sn-Bi solders have been performed even before the enforcement of RoHS Directive in 2003. Moon et al. (2001) found that when Sn-Bi solders are contaminated with Pb, the solidification behaviour of the solder changes and the freezing range of the solder will be increased. The Sn-58Bi solder alloys may have potential segregation issue during applications (Hansen & Anderko, 1993).

### **2.3. Creep**

#### **2.3.1. *Understanding creep and its importance***

Creep can be defined as the time-dependent deformation resulting from constant stress (ASTM International, 2012). Creep is most of the time an engineering concern for components with high operating temperatures and stresses. However, in certain material such as concrete, moderate creep can help to relieve tensile stresses and this helps to prevent cracking (Mallik, 2011). When the homologous temperature for a material exceeds 0.5, creep is of engineering significance (Mahmudi et al., 2013). The homologous temperature is the ratio of the temperature of a material to its melting temperature, with both temperatures in Kelvin scale. The eutectic Sn-58Bi solder alloy used in this study has a melting temperature of  $139^\circ\text{C}$ , and such a low melting point means that the material has a homologous temperature of 0.72 even at normal room temperature of  $25^\circ\text{C}$ . The high homologous temperature of the solder alloy means that its mechanical behaviour can be characterized using its creep performance.

#### **2.3.2. *Creep and semiconductor failures***

The Joint Electron Device Engineering Council (JEDEC), which is currently known as JEDEC Solid State Technology Association, was established in 1979 with the aim of developing a set of standards for semiconductor industry. The standards developed by JEDEC include industry standards, product standards and semiconductor failure standard test methods. Table 2.3.1 shows the list of typical semiconductor failure test methods developed by JEDEC.

Table 2.3.1 Typical JEDEC Tests for Component and Assembly Level Testing

(Source : JEDEC Solid State Technology Association, 2005)

Test #	Test
1a	Preconditioning
1b	Assembly for components on PWBs inc. Preconditioning
2	Unbiased HAST
3	High temp storage
4a	Temp Humidity Bias
4b	Temp Humidity No Bias
5	HAST with Bias
6	Temp Cycling
7	Power Temperature Cycling
8	Mechanical Shock (Drop Test)
9	Vibration, variable frequency
10	Bending, Monotonic & Cyclic
11	Solder Creep Rupture
12	Autoclave
13	Thermal Shock

Among all the tests listed in Table 2.3.1, the bending and solder creep rupture tests are the major tests where creep behaviour of the solder material plays a vital role. In semiconductor devices, creep mostly happen when temperature changes in the devices. Due to the different CTE possessed by different components in the devices, the components will expand and contract at different rate and this will subsequently cause the solders joining the components to deform. When the solder can no longer accommodate the creep damage, the joined components must deform or fracture, which will lead to the failure of the devices. Creep may impact solders by changing the shapes of the joints, causing excessive stress concentration in certain areas of the joints, coarsening of the grain of the solder material leading to reduction of joint strength, crack formation and finally leading to the failure of the devices. The effect of low creep performance of the solders can therefore lead to catastrophic failure of devices and machinery, and this may further lead to fatality. For instance, there was a case at Bialystok in Poland where the failure of a semiconductor diode caused

radiation injury to a patient. In that incident, the failure of diode has triggered a series of events which include failure of the control software of a medical radiotherapy equipment which then subsequently caused the particle accelerator of the equipment to malfunction and this led to overexposure of radiation on a patient (Holmberg, 2006; International Atomic Energy Agency, 2002).

#### *2.3.2.1. Solder crack*

With the presence of resistance in the circuit boards, it is inevitable that they will undergo temperature changes when current is passed through the circuit. The temperature changes may vary with different surrounding conditions and therefore the range of changes may be very large. In addition, the temperature changes are most of the time repetitive, and this subsequently causes the materials and components on the boards to undergo expansion and contraction. As different materials have different coefficient of thermal expansion (CTE), their rate of expansion and contraction will vary from each other. This will cause the solders joining the different materials and components to experience changes in stress concentration within the solders, which may cause cracks to develop in solder joints if the stress applied exceeds the stress limit. Solder crack is one of the major concerns in semiconductor industry as the failure of joint means the whole device will become dysfunctional. Solder cracks can be categorized into 3 different types based on the locations of the cracks, which are crack at interface, crack at IMC layer and crack at solder bulk.

##### *2.3.2.1.1. Interface crack*

Interface crack can be used to refer to the solder crack occurring at the interface between the components and the solders or between the substrate and the solders in electrical or electronic components. Figure 2.3.1 shows the typical locations of which interface cracks may occur.



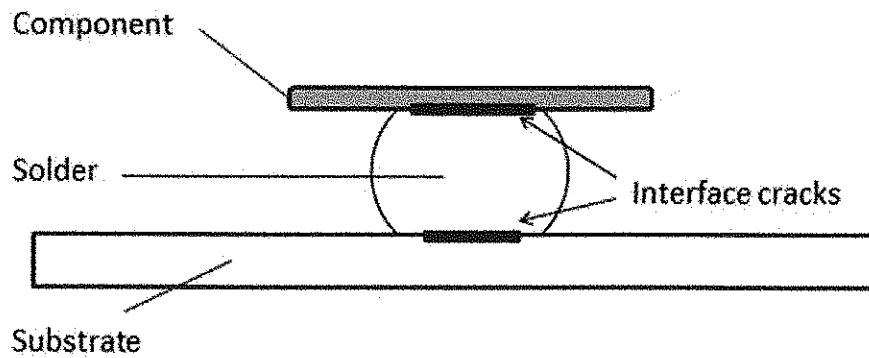


Figure 2.3.1 Possible locations of solder interface crack (indicated by thick bold lines)

Solder cracks at interface are mainly caused by sudden temperature change or thermal shock (Nishiura & Shiomi, 1992). When the solder is exposed to a sudden change in temperature, the thermal shock causes the solder material to undergo grain coarsening. With shear stress developed at the interface layer, the joint will fail when the stress developed exceeded the maximum limit. Wu (1998) found that when solder is cooled from its eutectic temperature to the room temperature, the cooling will initiate large residual displacement at the interface area of which the crack occurred. The thermal shock test is normally performed to detect solder interface crack in an electrical or electronic component. In addition, another method of using Non-Destructive Monitoring of Direct Current Potential Difference has been developed to evaluate the interface crack between a solder and its substrate (Tada, 2006 ; Andou & Tada, 2006). Using the Direct Current Potential Difference method, the crack is evaluated by the potential difference between the top of a wire placed into the solder material and the substrate.

#### 2.3.2.1.2. Crack at IMC Layer

IMC is a layer of compound formed near the interfaces of solders and the substrates or components during the soldering process. IMC layer is vital in producing a reliable joint between the solder and the component or substrate. IMC layer normally has hard and brittle properties, and the composition, structure and brittleness depend on the solder composition as well as the composition of the surface of substrate or component of which the joint is formed. Figure 2.3.2 shows the locations of which cracks may occur at IMC layers.

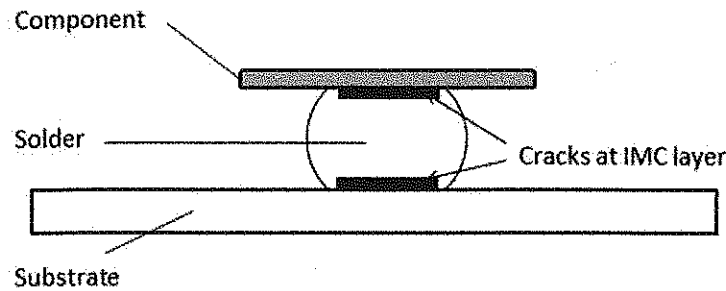


Figure 2.3.2 Possible locations of cracks at IMC layer of solder joints

Solder cracks at IMC layer may be caused by various factors such as rapid changes in temperature, mechanical shock, bending or even vibration. Most cracks occur due to high level of strain or high rate of low level strain being applied to the IMC layer (Tegehall, 2006).

The shear test and pull test with low strain rate are the conventional tests used to access the risk for cracks at brittle IMC layers (Coyle & Hodges Poppo, 2003; Li & Lee, 2002; Paik & Jeon, 2004; Zheng & Hillman, 2002). The results from the conventional tests, however, may be inaccurate in certain cases. For instance, cracks may only develop on nickel surfaces under high level of applied strain as well as high level of strain rate. This means that the conventional tests will show results indicating that brittle cracks may not happen but this may not be true when high strain level or high strain rate is applied. A few studies have been done and the results show that the conventional shear and pull tests are not adequate to test the risk for brittle cracks at the IMC layer (Chiu & Zeng, 2004; Date & Shoji, 2004; Newman, 2005; Sykes, 2005), as high strain level and high strain rate tests should be performed to access the risk for certain materials such as nickel. Besides the shear and pull tests, drop test may also be performed to access the risk of cracks developing at the IMC layer when the components experience mechanical shock.

#### 2.3.2.1.3. Crack at Solder Bulk

If the solder joints are properly formed, cracks will occur through the bulk of the solder itself if the stress applied to the solder has exceeded the limit (Westinghouse Defense & Space Center, 1968). Figure 2.3.3 shows a crack through the bulk of a solder.

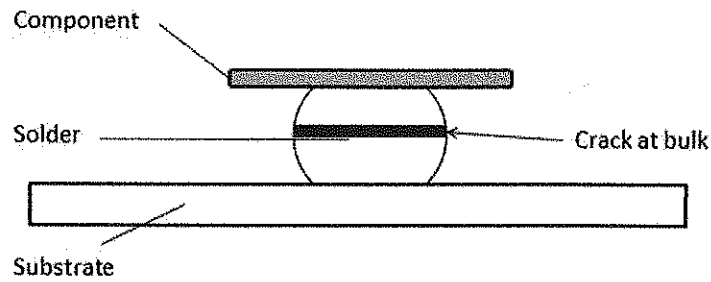


Figure 2.3.3 Possible crack location at the bulk of solder

The crack basically can occur at any areas within the solder bulk had the joints and the IMC layer near the interfaces between the solder and the component or the substrate are properly formed and are strong enough to withstand the stress applied. Cracks at solder bulk normally occur due to cyclic temperature changes and constant strain applied to the solder. The fatigue performance of the solder can be evaluated using thermal fatigue test while creep performance can be accessed using the Vickers hardness test which is being utilized in this research.

### 2.3.3. *Models developed for creep curves*

The three different stages of creep are primary creep, secondary creep and tertiary creep. The difference between these three stages can be observed from the creep curve shown in Figure 2.3.1, when the relationship between strain and time under constant load at fixed temperature is established. Primary creep represents the transient creep stage where the creep rate is decreasing. The creep rate will reach steady state due to the balance between recovery and strain hardening in the material, and this stage where the creep rate is minimum is also known as the secondary creep. The tertiary creep happens when the material is exposed to high temperature and high stresses, in this stage the creep rate will increase rapidly due to diffusion of particles, recrystallization or coarsening of precipitate particles (Mallik, 2011).

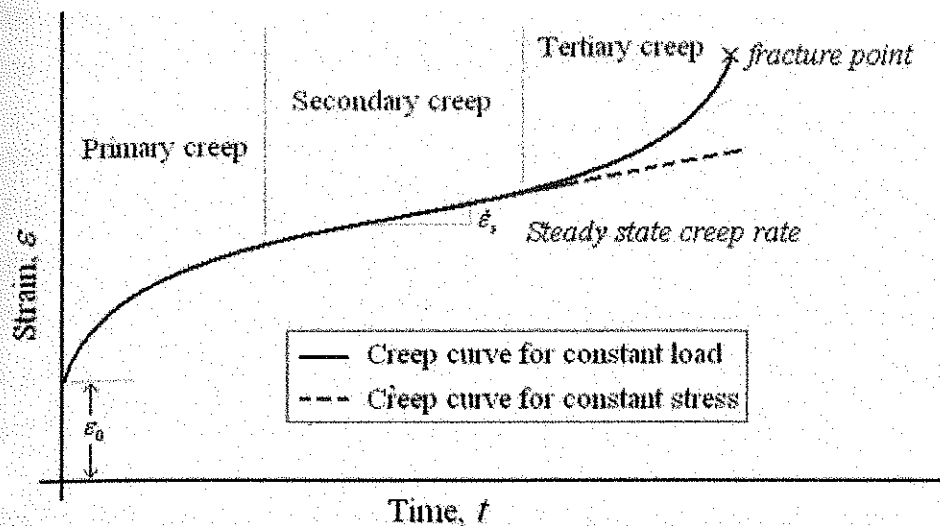


Figure 2.3.1 Strain vs time creep curves under constant load and constant stress

(Source : Kailas, 2013)

Various models have been developed to represent the deformation of materials at different stages of creep. For instance, Graham and Walles (1955) have developed a power law for primary creep of commercial alloy. Philips (1905) also developed a primary creep model equation for metal wires and rubber subjected to a constant pulling force, although his equation is different from Graham and Walles' power law in such a way that it is in logarithmic form. McVetty (1933) has also developed a primary creep equation in exponential form, while Conway and Mullikin (1962) provide another alternative for first stage creep analysis with a sinh law model equation.

The secondary creep is the most important design parameter to be considered if long-life application is one of the requirements. Two major models equation has been developed for this secondary stage where creep rate is the minimum. Norton (1929) developed a power creep law before Nadai (1938) developed a hyperbolic sine law to evaluate the secondary creep of materials.

The tertiary creep stage is normally evaluated due to concerns in rupture of the engineering materials under stresses. For short-life components, this stage of creep is the most important factor to be considered. McHenry (1943) initiated the development of an exponential tertiary creep equation and applied it in concrete

designs. His model was later being developed further by Kachanov (1958) and Rabotnov (1969) to solve for creep issues in structural members.

This study focuses on the secondary creep in which the creep rate is the minimum, as one of the properties that the solder material must possess is long-life application. The difference between the creep performance of the eutectic Sn-58Bi and the MWCNT-reinforced composites will be evaluated using the Sargent-Ashby model which is developed from Norton's power law (Sargent and Ashby, 1992). The Sargent-Ashby model focuses on analysis for indentation creep.

#### *2.3.4. Comparison between different types of creep tests*

Four major types of creep tests are widely used for characterizing the creep behaviour of engineering materials, these are conventional creep test, stress relaxation test, impression creep test and indentation creep test.

##### *2.3.4.1. Conventional creep, stress relaxation and impression creep*

The conventional creep lifting tests focuses on fully reproducing or predicting the full creep curve. Abdallah et al. (2014) have performed a critical analysis on the conventional creep lifting method used to characterize creep performance of a material and it was found that the Uniaxial Creep Lifting approach which yields a reasonable creep curve is the most suitable conventional method to be used for evaluating creep performance, but according to their review the approach still poorly estimated the primary creep curve. Various other approaches such as Larson-Miller, Manson-Haferd, Orr-Sherby-Dorn, Manson-Succop and Goldhoff-Sherby have also been developed to predict the creep curves but none of these can yield a good fit for the full creep curves (Abdallah et al., 2014).

The limitations on the conventional creep test have triggered the development of other types of creep tests to evaluate the creep behaviour of materials, one of which is the stress relaxation tests. The stress relaxation test is mainly used to characterize the creep behaviour of polymers and soft materials. During the test, the material will be subjected to tensile force at a fixed stress level. The decrease in load with time will be recorded and the load-time graph can be analysed with various types of analytical approaches to yield the stress exponents.

In impression creep test, a cylindrical punch with flat end is used to penetrate the material under constant load and temperature. The change in penetration depth with time will be recorded and the impression velocity obtained can be used for further analysis.

#### 2.3.4.2. Indentation creep

The indentation creep test is performed by using a hard indenter to penetrate a material under constant load and temperature. The load applied will be maintained over a period of time and the changes in size of the indentation are observed. The process is similar with impression creep test, as the variation in penetration depth with time will be analysed in characterizing the creep behaviour of the material. Indentation creep test is sometimes also known as nanoindentation test due to the tiny size of the residual impression, which can be as small as a few microns. The shape of the indenter may varies from spherical to pyramid, depending on the type of hardness test performed.

Although there are four major types of creep tests that can be applied for characterizing the creep behaviour of materials, the indentation test, or particularly the Vickers hardness test with pyramid indenter will be used for evaluating the creep performance of the materials in this study. Mahmudi et al. (2007) have performed a comparison between the four different types of creep tests using the Sn-40Pb-2.5Sb solder alloy with homologous temperature of more than 0.65, and it was found that the stress exponent values obtained from these creep tests are in good agreement with each other, with the values ranging from 2.55 to 3.20. It is therefore expected that when the experiment is repeated using other creep tests, the results yielded will be in good agreement with the results from the indentation test obtained through this study.

There are several advantages of using indentation creep technique to study the creep performance of the materials, one of which includes reduction in variation in property from sample to sample. This is due to the creep information can be obtained from the same piece of sample using the indentation creep technique unlike the conventional creep test, which may need more than one sample for the creep lifting test (Douglas et al., 1965). The indentation creep test is simple and non-destructive technique. This technique can also be applied to characterize the creep behaviour of intermetallic,